



**Universiteit
Leiden**
The Netherlands

A rare gain of function variant of hepatic lipase attenuates hypercholesterolaemia and atherosclerosis in mice via an LDL receptor-independent mechanism

Sotin, T.; Ge, X.K.; Schönke, M.; Vince, L.; Thouzeau, A.; Frey, S.; ... ; May, C. le

Citation

Sotin, T., Ge, X. K., Schönke, M., Vince, L., Thouzeau, A., Frey, S., ... May, C. le. (2025). A rare gain of function variant of hepatic lipase attenuates hypercholesterolaemia and atherosclerosis in mice via an LDL receptor-independent mechanism. *Cardiovascular Research*, 121(7), 1024-1035. doi:10.1093/cvr/cvaf097

Version: Publisher's Version

License: [Creative Commons CC BY 4.0 license](#)

Downloaded from: <https://hdl.handle.net/1887/4257841>

Note: To cite this publication please use the final published version (if applicable).

A rare gain of function variant of hepatic lipase attenuates hypercholesterolaemia and atherosclerosis in mice via an LDL receptor-independent mechanism

Thibaud Sotin ^{1†}, Xiaoke Ge ^{2†}, Milena Schönke ², Lucie Vince¹, Amélie Thouzeau¹, Samuel Frey ¹, Victoria Lorant¹, Lisa Krul², Amanda C.M. Pronk², Reshma Lalai², Trea C.M. Streefland², Salwa Afkir², Wieneke Dijk ^{1,3}, Sarra Smati¹, Marieke Heijink ⁴, Niek Blomberg⁴, Martin Giera ⁴, Mathilde Di Filippo ^{5,6}, Philippe Moulin ^{6,7}, Sander Kooijman ², Bertrand Cariou ^{1‡}, Patrick C.N. Rensen ^{2*‡}, and Cédric Le May ^{1*‡}

¹Nantes Université, CHU Nantes, CNRS, INSERM, l'institut du thorax, 8 quai Moncoussu, BP70721, Nantes F-44000, France; ²Department Medicine, Div. Endocrinology, and Einthoven Laboratory for Experimental Vascular Medicine, Leiden University Medical Center, P.O. Box 9600, Leiden 2300 RC, The Netherlands; ³INRAE, UR BIA, Nantes F-44316, France; ⁴Center for Proteomics and Metabolomics, Leiden University Medical Center, Leiden, The Netherlands; ⁵26900 Service de Biochimie et Biologie moléculaire, Laboratoire de Biologie Médicale Multi-sites, Hospices Civils de Lyon, Lyon Cedex, France; ⁶CarMen Laboratory, INSERM, INRA, INSA Lyon, Université Claude Bernard Lyon 1, Pierre-Bénite, France; and ⁷26900 Fédération d'endocrinologie, maladies métaboliques, diabète et nutrition, GHE, Hospices Civils de Lyon, Bron Cedex, France

Received 16 January 2025; revised 5 March 2025; accepted 24 March 2025; online publish-ahead-of-print 3 June 2025

Time of primary review: 26 days

Aims

LIPC encodes hepatic lipase (HL), a liver-bound protein with both phospholipase and triglyceride lipase activity, and involved in the catabolism of circulating lipoproteins. We recently identified the gain-of-function variant HL-E97G, with selectively increased phospholipase activity, as a new genetic cause of familial combined hypocholesterolaemia in humans. The role of HL in the development of atherosclerosis remains controversial. In this context, the action of HL-E97G on the development of atherosclerosis remains unknown.

Methods and results

To evaluate the lipid-lowering and anti-atherogenic properties of HL-E97G vs. wildtype HL (HL-WT) in hypercholesterolaemic *APOE*3-Leiden.CETP* mice, a well-established model for human-like lipoprotein metabolism, and to assess dependence of these effects on the LDL receptor (LDLR) pathway in LDLR-deficient (*Ldlr*^{-/-}) mice. *APOE*3.Leiden.CETP* mice or *Ldlr*^{-/-} mice received an intravenous injection of AAV8 expressing either eGFP (control), HL-WT or HL-E97G (3×10^{11} GC/mouse) while being fed pro-atherogenic diets. Plasma cholesterol levels were measured monthly, and aortic atherosclerotic lesion sizes were assessed at termination. HL-E97G largely decreased plasma total cholesterol exposure in *APOE*3-Leiden.CETP* mice (−63% vs. control; −58% vs. HL-WT), resulting at least in part from increased uptake of (V)LDL by the liver, accompanied by a marked decrease in atherosclerotic lesion size (−98% vs. control; −97% vs. HL-WT) in the aortic root. Importantly, HL-E97G also strongly reduced plasma cholesterol exposure in *Ldlr*^{-/-} mice (−80% vs. control; −77% vs. HL-WT), and decreased atherosclerotic lesion size in the aortic root (−54% vs. control; −41% vs. HL-WT) and the aortic arch (−73% vs. control; −70% vs. HL-WT).

Conclusions

HL-E97G strongly reduces plasma cholesterol levels, by increasing the uptake of (V)LDL, to decrease atherosclerosis development in mice independently of the LDLR pathway. These data suggest that modulating HL function is a promising tool in patients with familial hypercholesterolaemia.

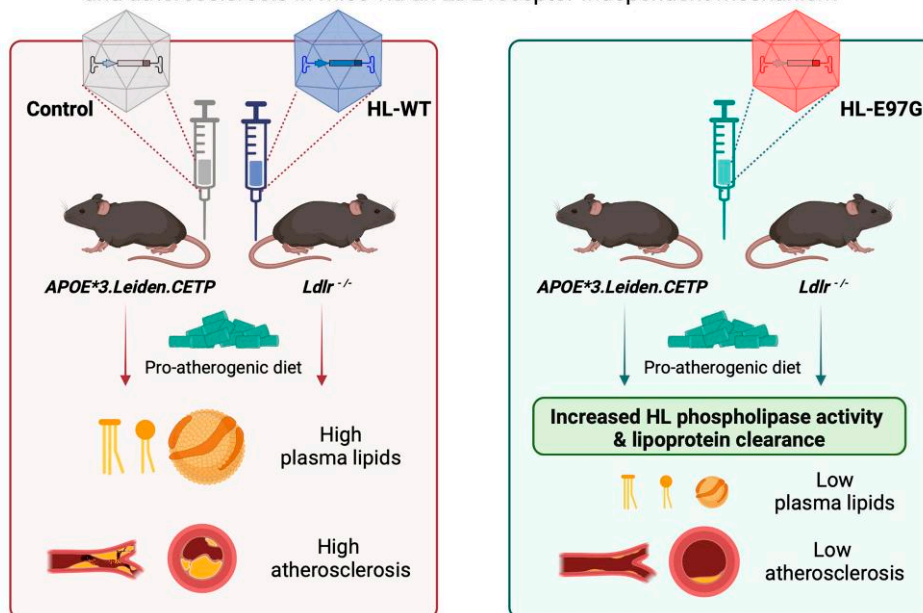
* Corresponding author. Tel: +31 (0)71 52 63078, E-mail: p.c.n.rensen@lumc.nl (P.C.N.R.); Tel: +33 (0)2 28 08 01 69, E-mail: cedric.lemay@univ-nantes.fr (C.L.M.)

† Co-first authors.

‡ Co-senior authors.

Graphical Abstract

A rare gain of function variant of hepatic lipase (HL-E97G) attenuates hypercholesterolemia and atherosclerosis in mice via an LDL receptor-independent mechanism



Keywords

Hepatic lipase • Atherosclerosis • Familial combined hypocholesterolaemia • HL-E97G

1. Introduction

Atherosclerotic cardiovascular disease (ASCVD) is the leading cause of premature death worldwide, accounting for as many as 20 million deaths annually.^{1,2} Dyslipidaemia, particularly elevated low density lipoprotein cholesterol (LDL-C) concentration, remains one of the most important modifiable risk factors for ASCVD.³ Exposure to lower cumulative concentrations of LDL-C in young or middle-aged individuals is associated with a reduction in long-term ASCVD risk.⁴ In addition, the results of cardiovascular outcomes randomized trials with powerful lipid-lowering therapies (LLTs), such as proprotein convertase subtilisin/kexin type 9 (PCSK9) inhibitors, have led to a progressive lowering of the LDL-C target for the prevention of ASCVD in international guidelines, reaching 55 mg/dL (1.4 mM) for patients at highest risk.⁵ However, a significant proportion of individuals, especially those at very high risk of ASCVD, do not achieve LDL-C targets due to treatment intolerance, low compliance, or ineffectiveness despite the emergence of numerous innovative therapeutic solutions in recent years.^{6,7}

In this context, a particular clinical situation is that of homozygous familial hypercholesterolaemia (HoFH), a rare disease characterised by very high concentrations of LDL-C and premature atherosclerosis occurring from childhood onwards in the absence of management.⁸ Since patients with HoFH can have no residual LDL receptor (LDLR) function according to the severity of mutation, the standard LLTs (i.e. statins and PCSK9 inhibitors) are either ineffective or only marginally effective because their mode of action is through up-regulation and stabilization of the LDLR.^{9,10} Recently, a randomized controlled trial demonstrated that evinacumab, an inhibitor of angiopoietin-like 3 protein (ANGPTL3) was safe and effective in all HoFH subgroups.^{8,11} Lomitapide, an inhibitor of microsomal triglyceride transfer protein, was also reported to reduce LDL-C levels in HoFH, but issues with adverse events (i.e. liver steatosis), tolerability with gastrointestinal disturbances, and adherence were identified.¹⁰ Finally, in these

HoFH patients, weekly or twice-weekly LDL-apheresis remains an essential therapeutic strategy.

Interestingly, we recently identified a novel rare variant in the *LIPC* gene (HL-E97G) in a large pedigree of individuals with both low LDL-C and high density lipoprotein cholesterol (HDL-C) concentrations as a genetic cause of familial combined hypolipidaemia.¹² *LIPC* encodes hepatic lipase (HL), which belongs to the family of glycerol-sn-1 fatty acid hydrolases that includes lipoprotein lipase (LPL) and endothelial lipase (EL).¹² HL has a balanced hydrolytic activity for both triglycerides (TG) and phospholipids (PL),^{12,13} and plays an important role in lipoprotein metabolism by catabolizing HDL-C and TG-rich lipoproteins (reviewed in Santamarina-Fojo *et al.*¹³). We showed that HL-E97G is a gain-of-function variant of HL with selectively increased phospholipase activity.¹² Hepatic expression of HL-E97G in male *APOE*3.Leiden.CETP* mice reduces plasma PL, TG, and cholesterol levels compared to HL-WT, mimicking the combined hypolipidaemia observed in individuals who carry the HL-E97G variant.¹²

Given that the proband in the family had revascularized coronary artery disease¹² and the significant drop in HDL-C, it was important to determine the impact of the HL-E97G variant on the development of atherosclerosis. Here, we investigated the effect of hepatic expression of HL-E97G vs. HL-WT on atherosclerosis development in hypercholesterolaemic *APOE*3.Leiden.CETP* mice, a well-established model of human lipoprotein metabolism, and also in LDLR-deficient (*Ldlr^{-/-}*) mice in order to determine the importance of the LDLR pathway in the effects of the HL-E97G variant.

2. Methods

2.1 Mouse studies

*APOE*3-Leiden.CETP* mice (C57Bl/6) background) were bred at Leiden University Medical Center (Leiden, The Netherlands), and used for

experiments as approved by the Animal Welfare Body Leiden and executed under a license granted by the Central Authority for Scientific Procedures on Animals (CCD) under the license number AVD11600202010187 in accordance with the Dutch Act on Animal Experimentation and EU Directive 2010/63/EU. *Ldlr*^{-/-} mice (C57Bl/6j background) were bred at Nantes Université animal facility (Nantes, France), and used for experiments as approved by the ethics committee of Pays de la Loire (France, 006) and the Ministère de l'Enseignement supérieur et de la Recherche (France; APAFIS 26862). All mice were group housed under a 12 h light–dark cycle, at 22°C, and had free access to water and food unless indicated otherwise.

In a first experiment, *APOE**3-*Leiden.CETP* mice (8–14 weeks old) were fed a Western-type diet (Ssniff Spezialdiäten GmbH, Germany) containing 16% fat and 0.15% cholesterol. We used females only as males fail to increase circulating cholesterol on a Western-type diet and develop only very small lesions.¹⁴ Following a 3-week dietary run-in period to induce hyperlipidaemia, mice were assigned to blocks ($n = 16$ per group) that were balanced for plasma total cholesterol (TC), TG, PL, and body weight using RandoMice.¹⁵ Groups were randomly assigned to receive an intravenous injection with 3×10^{11} genome copies of adeno-associated viruses (AAV8) expressing, under the thyroxin-binding globulin (TBG) promoter, either enhanced green fluorescent protein (eGFP; control), the human *LIPC* gene encoding wildtype HL (HL-WT), or the human *LIPC* gene encoding the gain-of-function E97G variant of HL (HL-E97G) (Vector Biolabs, USA).

In a second experiment, male and female *Ldlr*^{-/-} mice (10–14 weeks old) were block-randomized into three groups ($n = 8$ –10 per group) balanced for plasma TC, TG, and body weight using RandoMice,¹⁵ and fed with a pro-atherogenic diet containing 17% cocoa butter, 1.25% cholesterol, and 0.5% cholic acid (Research Diet #D12109Ci, USA). Upon switching to this diet, mice received intravenous injections of the same viruses at the same dose as the *APOE**3-*Leiden.CETP* mice.

2.2 Body weight, organ weight, and blood biochemistry

Mice were weighed on a weighing scale every 4–6 weeks. Blood was collected from the mouse tail after 4 h of fasting (from 9 am to 1 pm) every 4–6 weeks using paraoxon-coated capillaries, and plasma was obtained through centrifugation.

In *APOE**3-*Leiden.CETP* mice, the weight of organs/tissues, including liver, gonadal white adipose tissue (gWAT), subcutaneous white adipose tissue (sWAT), interscapular brown adipose tissue (iBAT), subscapular brown adipose tissue (sBAT), spleen, kidneys heart, and adrenals were measured at the end of the experiment. Plasma levels of TC, TG, and PL were measured using enzymatic kits (Roche Diagnostics, Germany). Lipoprotein profiles were determined from pooled plasma samples collected at Week 16 (equal plasma volumes per mouse of each group) by fast protein liquid chromatography (FPLC) with a Superose 6 column (Cytiva, USA), followed by measurement of PL, TG, and TC levels in the obtained fractions by enzymatic kits (Roche Diagnostics, Germany). Plasma HDL-C and HDL-PL levels were measured in the supernatant after precipitating ApoB-containing lipoproteins as previously described,¹⁶ using the enzymatic kit for TC and PL (Roche Diagnostics, Germany).

In *Ldlr*^{-/-} mice, the plasma levels of TC, TG, PL, and HDL-C were measured using colorimetric assays (TC&TG: SOBIODA, France; PL: Phospholipids FS, DiaSys; HDL-C: HDL-C direct FS, DiaSys). Non-HDL-C levels were calculated by subtracting HDL-C from TC.

Plasma TC exposure was determined by calculating the area under the curve of plasma TC levels over the experimental period.

2.3 In vivo organ/tissue uptake of VLDL-like particles and LDL

In *APOE**3-*Leiden.CETP* mice, at 17 weeks after virus injection, subgroups of mice ($n = 8$) with body weight and plasma lipids close to the group mean were intravenously injected with glycerol tri[³H]oleate ([³H]TO) and [¹⁴C]cholesteryl oleate ([¹⁴C]CO) double-labelled very low density

lipoprotein (VLDL)-like particles (1.0 mg TG in 200 μ L saline per mouse) or [³H]TO and [¹⁴C]CO double-labelled human LDL (0.2 mg TC in 200 μ L saline per mouse) as described before.¹² Mice were killed by CO₂ inhalation at 15 min after injection of VLDL-like particles or at 30 min after injection of LDL and perfused with ice-cold PBS before organs/tissues were collected. Samples were dissolved overnight at 55°C in Solvable (PerkinElmer, The Netherlands) and then were mixed with Ultima Gold liquid scintillation cocktail (PerkinElmer, The Netherlands). ³H and ¹⁴C activity in the samples (disintegrations per min) were measured using a Tri-Carb 2910TR low-activity liquid scintillation analyser (PerkinElmer, The Netherlands). The uptake of ³H and ¹⁴C radioactivity by the organs/tissues was expressed as the percentage of injected radioactive dose.

2.4 Faecal cholesterol and faecal bile acid quantification

In *APOE**3-*Leiden.CETP* mice, at 10 weeks after virus injection, faeces were collected during 48 h to determine lipid excretion. After freeze-drying, faecal samples were homogenized in 90% isopropanol at 0.05 mg/ μ L. To 5 μ L of this homogenate, 10 μ L 400 μ g/mL cholesterol-d7 (Avanti, USA) in ethanol (Merck, USA), 10 μ L water (Honeywell Riedel-de Haën, Germany), and 65 μ L ethanol was added. Subsequently, samples were hydrolyzed at 70°C for 1 h by adding 10 μ L 10 M sodium hydroxide (Sigma Aldrich, USA). Cholesterol was extracted on a Strata™-X 33 μ m Polymeric Reverse Phase solid phase 1 mL extraction tube (Phenomenex, USA). The cartridge was activated with methanol (Merck, USA), and equilibrated with water, after which the sample was loaded. Thereafter, samples were washed with water, eluted using methyl formate (Sigma Aldrich, USA) and the combined organic extract was dried. Cholesterol was derivatized by adding 50 μ L *N*-methyl-*N*-trimethylsilyltrifluoroacetamide containing 1% trimethylchlorosilane (Thermo Fisher Scientific, USA) and 10% *N*-trimethylsilyl-imidazole (Thermo Fisher Scientific, USA). Finally, 150 μ L tert-butyl methyl ether (Sigma Aldrich, USA) was added. Samples were analysed on a gas chromatograph (8890 GC system; Agilent, USA) coupled to a mass spectrometer (5977B GC/MSD; Agilent, USA) equipped with an electron ionization source. Samples (1 μ L) were injected splitless at 300°C. Cholesterol was separated on a VF-5 ms column (Agilent, USA), and helium was used as carrier gas at a flow of 1 mL/min. The oven was set as follows: 1 min at 175°C, increase to 290°C at 50°C/min, increase to 310°C at 5°C/min, 5.7 min at 310°C. The transfer line was set at 280°C, the source at 230°C, and the quadrupole at 150°C. For cholesterol-d7 *m/z* 336.4 (quantifier), 375.4, 465.5 and for cholesterol *m/z* 459.4 (quantifier), 354.3, 444.4 were used. Cholesterol was quantified using an external calibration line.

Bile acids in faeces were analysed as described elsewhere¹⁷ with minor modifications. Dried faeces were homogenized in 75% MeOH (4 mg/mL), and the homogenate was centrifuged at 18 213 g for 5 min at 20°C. The supernatant was taken, 4 μ L, and spiked with 20 μ L internal standard solution (500 ng/mL) and further diluted by the addition of 90 μ L MeOH and 90 μ L water. The samples were measured using a Shimadzu Nexera LC40 system, consisting of a DGU-405 degasser, two LC-40D X3 pumps, a SIL-40C X3 autosampler, and a CTO-40S column oven (Shimadzu, USA). The gradient used was as follows: 0–0.2 min, constant at 20% B; 0.2–0.5 min, linear increase to 49% B; 0.5–5.5 min, linear increase to 64% B; 5.5–7.9 min, linear increase to 100% B; 7.9–9.9 min, constant at 100% B.

2.5 Liver histology and lipid content

In *APOE**3-*Leiden.CETP* mice, liver samples were collected and fixated with phosphate-buffered formaldehyde and embedded in paraffin and cross-sectioned (5 μ m thickness). Sections were stained with haematoxylin–eosin (HE) and the lipid area was quantified using ImageJ software v1.52a. Hepatic lipids were extracted from snap-frozen liver samples according to a modified method from Bligh and Dyer.¹⁸ Hepatic TG and TC levels were measured using enzymatic kits (Roche Diagnostics, Germany). Hepatic protein concentrations were measured using a BCA

Protein assay kit (Thermo Fisher Scientific, USA). Hepatic lipid levels were expressed as nmol per mg protein.

2.6 Gene expression analysis

Total RNA was isolated from snap-frozen liver, sWAT, or aorta samples with TriPure RNA Isolation Reagent (Sigma Aldrich, USA), and the concentration of isolated RNA was determined by Nanodrop technology (Thermo Fisher Scientific, USA). Then, 1 µg RNA of each sample was reverse-transcribed into cDNA using Moloney murine leukaemia virus reverse transcriptase (Promega, USA). Quantitative real-time PCR was performed using the GoTaq Real-Time PCR Detection Master Mix (Promega, USA) on a CFX386 machine (Bio-Rad, USA) according to the manufacturer's protocol. The expression of mRNA level was normalized to beta-actin (*Actb*) and glyceraldehyde-3-phosphate dehydrogenase (*Gapdh*) mRNA expression and expressed as fold change compared with the eGFP or WT-LIPC group using the 2 to the power of $-\Delta\Delta C_t$ method. The primer sequences are listed in [Supplementary material online, Table S1](#).

2.7 Atherosclerosis visualization and quantification

At 17 weeks after virus injection into *APOE*3-Leiden.CETP* mice, mice were killed by CO₂ inhalation followed by heart puncture and then perfused with ice-cold PBS. Hearts were collected, fixed in phosphate-buffered formaldehyde, and then embedded in paraffin. After cross-sectioning (5 µm thickness) throughout the aortic root area, four consecutive sections per heart at 50 µm intervals (starting at the opening of the aortic valves) were treated with haematoxylin phloxine saffron (HPS) to stain macrophages/nuclei/cellular components (haematoxylin; blue-purple), smooth muscle cells/cytoplasm (phloxine; pink-red), and collagen/fibrous caps (saffron; yellow) within atherosclerotic lesions. According to the guidelines of the American Heart Association adapted for mice,^{19,20} lesions were categorized into mild lesions (types I–III) or severe lesions (type IV–V). Smooth muscle cells were stained using an anti- α -actin antibody (1:1000 dilution; Dako, Denmark) and a secondary antibody EnVision System-Horseradish peroxidase Labeled Polymer (1:400 dilution; Dako, Denmark) that was visualized by Liquid DAB + Substrate Chromogen System (Dako, Denmark). Collagen was stained with Sirius Red (Sigma Aldrich, USA). Macrophages were stained with an anti-Mac-3 antibody (1:1000 dilution; BD Pharmingen, USA), a horseradish peroxidase-labelled secondary antibody and a peroxide substrate (1:400 dilution; Vector Laboratories, USA). Stained slides were scanned with a 3DHistech Panoramic 250 Flash III DX (3DHistech, Hungary). Lesion areas and the areas of smooth muscle cells, collagen, and macrophages were quantified using ImageJ software v1.52a. The lesion stability index was calculated as the ratio of stable markers (i.e. smooth muscle cell area and collagen area) per unstable marker (i.e. macrophage area).

At 14 weeks after virus injection, *Ldlr*^{-/-} mice were anesthetized with ip injection of a mixture of ketamine (100 mg/kg) and xylazine (20 mg/kg) followed by heart puncture and then perfused with ice-cold PBS. The aortic arches, with the major arteries that stem from them (brachiocephalic, left common carotid and left subclavian), were dissected under a microscope, frozen in optimal cutting temperature medium (O.C.T.; Sakura, USA) and stored at -80°C before serial cryo-sectioning. The aortic roots were dissected under a microscope and frozen in O.C.T. medium and stored at -80°C before serial cryo-sectioning and oil red O staining. Cryostat sections were cut at -20°C using a CryoStar NX70 cryostat (Thermo Fisher Scientific, USA). Sections of 5 µm thickness were harvested (when the three arteries were visible of the aortic arches; when the three aortic valve leaflets were visible of the aortic roots), mounted on SuperFrost Plus glass slides (Thermo Fisher Scientific, USA), and stored at -80°C until use as described.²¹ Oil red O (Sigma Aldrich, USA) was used to stain neutral lipids according to the protocol of Mehlem et al.²² Stained slides were scanned with a Hamamatsu C9600-12 NanoZoomer HT Scanner

(Hamamatsu, Japan) within 24 h. The lesion area was quantified using NDP.view2 software (Hamamatsu, Japan).

2.8 Statistical analysis

Data were analysed by GraphPad Prism Software v9.3.1. A one-way ANOVA with a Tukey correction for multiple comparisons was used for comparing the effects of treatments. Data are shown as mean \pm S.E.M. $P < 0.05$ was considered significant.

3. Results

3.1 HL-E97G improves dyslipidaemia in *APOE*3-Leiden.CETP* mice fed with a Western-type diet

Female *APOE*3-Leiden.CETP* mice were fed a Western-type diet were injected intravenously with AAV8-TGB-eGFP (control), AAV8-TGB-LIPC (HL-WT), or AAV8-TGB-LIPC E97G (HL-E97G) (Figure 1A). HL-E97G and HL-WT, but not control virus injection, resulted in expression of human LIPC (*hLIPC*) in the liver (Figure 1B), but not in other extrahepatic tissues such as sWAT (see [Supplementary material online, Figure S1A](#)) and aorta (see [Supplementary material online, Figure S1B](#)). The expression of HL-E97G and HL-WT did not affect hepatic expression of endogenous mouse *LipC* (*mLipC*; Figure 1C). HL-E97G and HL-WT did not affect body weight (Figure 1D) and the weight of organs/tissues (Figure 1E). In line with its specifically enhanced phospholipase activity (see [Supplementary material online, Figure S1C and D](#)),¹² HL-E97G induced a profound and sustained reduction in plasma PL compared to the control group (-40% vs. control; -22% vs. HL-WT at Week 16; Figure 1F) and an increased lysophospholipid/phospholipid ratio, while HL-WT was marginally effective (-24% vs. control; Figure 1F). Likewise, HL-E97G induced a profound reduction in plasma TG (-44% vs. control; -31% vs. HL-WT; Figure 1G) and TC (-48% vs. control; -30% vs. HL-WT; Figure 1H), while HL-WT was much less effective. FPLC profiling of pooled plasma showed that HL-E97G mainly reduced PL, TG, and TC within (V)LDL fractions (Figure 1I–K). In fact, the decrease in TC by HL-E97G was explained by a major decrease in non-HDL-C (-50% vs. control; -32% vs. HL-WT; Figure 1L) and a milder decrease in HDL-C (-24% vs. control; Figure 1M) without changing the gross composition of HDL (i.e. cholesterol and phospholipid; [Supplementary material online, Figure S1E and F](#)). HL-E97G largely decreased TC exposure (i.e. the area under the curve of cholesterol during 16 weeks) vs. both control (-63%) and HL-WT (-58%) (Figure 1N).

3.2 HL-E97G increases V(LDL) uptake by liver in *APOE*3-Leiden.CETP* mice

To directly evaluate the effect of HL-E97G on lipoprotein kinetics, we intravenously injected *APOE*3-Leiden.CETP* mice with either VLDL-like particles (Figure 2A–D) or human LDL (Figure 2E–H) that were labelled with [³H]TO and [¹⁴C]CO. For both VLDL-like particles and LDL, HL-E97G increased the uptake of [³H]TO and [¹⁴C]CO by the liver, while HL-WT did not (Figure 2A, C, E, and G). HL-E97G also slightly increased the uptake of [³H]TO and [¹⁴C]CO from LDL by spleen, heart, sBAT, and adrenals (Figure 2B, D, F, and H). These data suggest that HL-E97G reduces plasma lipids in part by increasing (V)LDL uptake by the liver, with a plausible additional contribution from extrahepatic tissues.

3.3 HL-E97G does not affect hepatic lipid content and faecal lipid excretion in *APOE*3-Leiden.CETP* mice

Since HL-E97G increased (V)LDL uptake by the liver, we next investigated the impact on liver lipids. HL-E97G and WL-WT did not affect liver histology (Figure 3A), hepatic lipid area (Figure 3B), or hepatic contents of TG (Figure 3C), TC (Figure 3D), and PL (Figure 3E). Likewise, HL-E97G

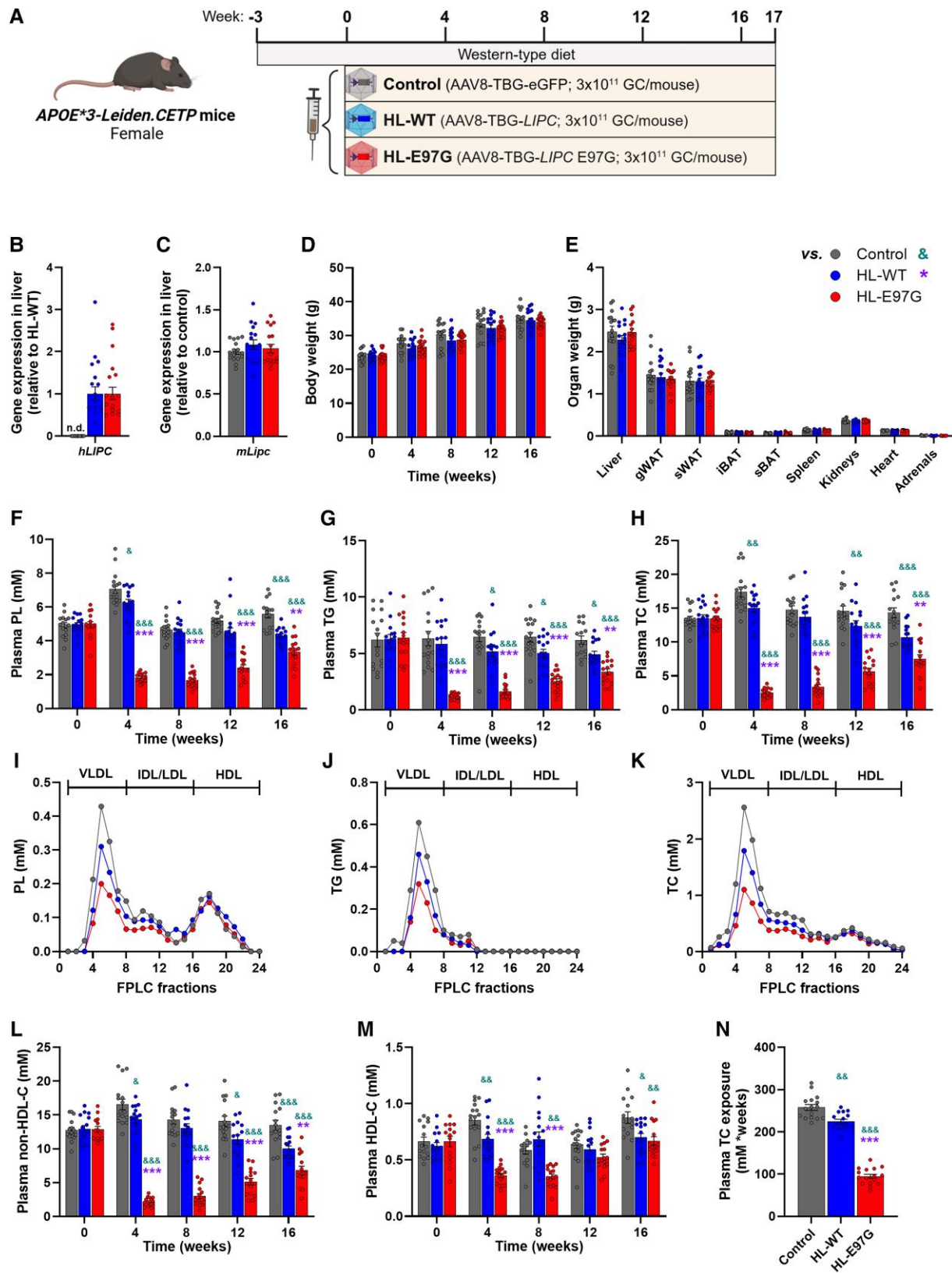


Figure 1 Human HL-E97G expression reduces plasma phospholipid, triglyceride, and cholesterol levels in *APOE*3.Leiden.CETP* mice. *APOE*3.Leiden.CETP* mice fed a Western-type diet received an intravenous injection with 3×10^{11} genome copies (GC) of adeno-associated viruses (AAV8) expressing either enhanced green fluorescent protein (eGFP; control), the human *LIPC* gene encoding wildtype HL (HL-WT), or the human *LIPC* gene encoding the gain-of-function E97G variant of HL (HL-E97G). Throughout the experimental period, 4 h fasted blood samples were collected to obtain plasma (at Weeks 0, 4, 8, 12, and 16) (continued)

Figure 1 Continued

and mice were killed after 17 weeks of virus injection and organs/tissues were collected (A). Hepatic expression of human HL (*hLIPC*; B) and mouse HL (*mLipC*; C) were determined. Body weight (D) and organ weight (E) were recorded. Plasma levels of phospholipids (PL; F), triglycerides (TG; G), and total cholesterol (TC; H) were determined. In pooled plasma samples collected at Week 16, lipoproteins were separated by fast protein liquid chromatography (FPLC) to measure PL (I), TG (J), and TC (K) levels in collected fractions. Plasma non-high density lipoprotein cholesterol (non-HDL-C; L) and HDL-C (M) levels were measured. Plasma TC exposure (N) was calculated from TC levels throughout the experimental period. Data are shown as mean \pm S.E.M. (B–H and L–N, $n = 14$ –16/group). Differences were assessed using one-way ANOVA with a Tukey correction for multiple comparisons. $^{\&P} < 0.05$, $^{\&\&P} < 0.01$, $^{\&\&\&P} < 0.001$, compared with the control group. $^{**P} < 0.01$, $^{***P} < 0.001$, compared with the HL-WT group. gWAT, gonadal white adipose tissue; HL, hepatic lipase; *hLIPC*, human hepatic lipase; iBAT, interscapular brown adipose tissue; *mLipC*, mouse hepatic lipase; sBAT, subscapular brown adipose tissue; sWAT, subcutaneous white adipose tissue.

did not affect excretion of faeces (Figure 3F), faecal cholesterol (Figure 3G), and faecal bile acids contents (Figure 3H), suggesting that HL-E97G does not affect lipid excretion. Also, HL-E97G did not alter the hepatic expression of genes involved in lipogenesis, cholesterol synthesis, or VLDL production (Figure 3I), suggesting that HL-E97G does not affect VLDL production. While HL-E97G increased (V)LDL uptake by the liver, hepatic expression of *Pcsk9* and *Ldlr* was not affected (Figure 3J). Collectively, these data indicate that HL-E97G does not induce liver steatosis and toxicity.

3.4 HL-E97G decreases atherosclerotic lesion area and severity in *APOE*3-Leiden.CETP* mice

Since HL-E97G largely reduced plasma TC, the most important risk factor for atherosclerosis, we next determined the atherosclerotic lesion size in the aortic root at 17 weeks after virus injection. Representative examples of HPS-stained sections are shown in Figure 4A. HL-E97G profoundly decreased the atherosclerotic lesion size throughout the aortic root (Figure 4B), resulting in a significant reduction of the average lesion size (-98% vs. control; -97% vs. HL-WT; Figure 4C) while HL-WT did not significantly affect lesion size (Figure 4B and C). Further characterization of lesions revealed that HL-E97G largely increased the percentage of unaffected sections (4-fold vs. control; 5-fold vs. HL-WT; Figure 4D), with 7/16 mice devoid of lesions. In fact, the lesions that were present in the HL-E97G expressing mice were all mild, compared with 35% severe lesions in controls and HL-WT expressing mice (Figure 4E). Next, the composition of lesions was determined (i.e. smooth muscle cell and collagen as stability markers of lesions; macrophage as instability marker of lesions) (Figure 4F) to reveal that although HL-E97G did not grossly affect lesion composition (Figure 4G), it improved the lesion stability index (i.e. sum of smooth muscle cell and collagen area divided by macrophage area) of type III lesions (Figure 4H). Taken together, our data show that HL-E97G but not HL-WT markedly attenuates atherosclerotic lesion development in *APOE*3.Leiden.CETP* mice.

3.5 HL-E97G improves dyslipidaemia and reduces atherosclerosis in *Ldlr*^{-/-} mice

To assess whether the lipid-lowering effect of HL-E97G is dependent on the LDLR pathway, we next evaluated the effects of HL-E97G vs. HL-WT on plasma lipids and atherosclerosis development in *Ldlr*^{-/-} mice. To this end, male and female *Ldlr*^{-/-} mice fed with a pro-atherogenic diet received an intravenous injection of AAV8-TGB-eGFP (control), AAV8-TGB-LIPC (HL-WT), or AAV8-TGB-LIPC E97G (HL-E97G) (Figure 5A). Similar to *APOE*3-Leiden.CETP* mice, HL-E97G did not affect body weight (Figure 5B) and markedly reduced plasma PL (-75% vs. control; -68% vs. HL-WT; Figure 5C), plasma TG (-89% vs. control; -80% vs. HL-WT; Figure 5D), and TC levels (-79% vs. control; -77% vs. HL-WT at Week 14; Figure 5E) in *Ldlr*^{-/-} mice. HL-E97G also decreased both non-HDL-C (-86% vs. control; -83% vs. HL-WT; Figure 5F) and HDL-C (-69% vs. control; -66% vs. HL-WT; Figure 5G) levels. Similar to *APOE*3-Leiden.CETP* mice, HL-E97G markedly reduced plasma TC exposure (-80% vs. control; -77% vs. HL-WT) in *Ldlr*^{-/-} mice (Figure 5H).

Next, we measured atherosclerotic lesion size in both the aortic root and aortic arch after 14 weeks of virus injection. Representative examples of oil Red O-stained sections are shown for the aortic root (Figure 5I) and aortic arch (Figure 5K). While HL-WT did not reduce or worsen aortic atherosclerotic lesions compared to the control group in the aortic root (Figure 5J) or arch (Figure 5L), HL-E97G reduced the lesion area in the aortic root lesions (-54% vs. control; -41% vs. HL-WT; Figure 5J) and even more strongly in the aortic arch (-73% vs. control; -71% vs. HL-WT; Figure 5L). Although small group sizes precluded statistical analysis in males and females separately, HL-E97G seemed to consistently reduce plasma lipids and atherosclerotic lesion area in both sexes (see Supplementary material online, Figure S2A–I).

These data demonstrate for the first time that HL-E97G reduced plasma lipids independent of the LDLR pathway and can effectively delay and reduce the progression of atherosclerosis in mice lacking LDLR.

4. Discussion

The HL-E97G variant leading to a specific increase in HL phospholipase activity was recently identified in a family with combined hypocholesterolaemia phenotype characterized by a fall in both plasma LDL-C and HDL-C concentrations.¹² The functional characterization performed in this study has allowed us to extend our knowledge of this variant. We have shown for the first time that HL-E97G not only lowers cholesterol levels, in part through increased hepatic uptake of (V)LDL, but also significantly prevents atherosclerotic lesions, in contrast to the wildtype form of HL. We also demonstrate that HL-E97G exerts its cholesterol-lowering action independently of LDLR and that it is also able of protecting *Ldlr*^{-/-} mice from atherosclerosis. These data validate the extreme therapeutic interest of HL-E97G for the treatment of hypercholesterolaemia, particularly the most severe forms such as HoFH.

The role of HL in the development of atherosclerosis remains a subject of debate. On the one hand, HL lowers HDL-C and increases small dense LDL concentrations, both of which can contribute to atherosclerosis.^{23,24} On the other hand, HL can also exert anti-atherogenic properties by promoting the clearance of lipoprotein remnants and potentially the reverse cholesterol transport by increasing β -HDL levels.^{25–27} In *Ldlr*^{-/-} mice, the genetic deletion of HL promotes the premature development of atherosclerotic plaques.²⁸ Conversely, transgenic re-expression of HL in either *Ldlr*^{-/-} or apolipoprotein E knockout mice significantly reduces atherosclerotic plaque development, and this effect is dependent on the enzymatic functions of HL.^{26,28} Genetic data have failed to clarify the role of HL, with again discordant results according to study populations. Individuals with complete HL deficiency are very rare and some of these individuals did develop ASCVD whereas other did not.^{13,25,29} However, low HL activity was associated with an increased risk of coronary heart diseases.³⁰ In accordance with this observation, a Mendelian randomization study demonstrated that low HL activity was causally related to higher ASCVD risk,³¹ but this has not been confirmed in other similar studies using the same genetic variant.^{32,33} Thus, while there is a tendency towards a negative association between HL activity and ASCVD risk, this effect is modest and not always consistent. In the present study, expression of the wildtype form of HL had indeed a much more modest effect on total

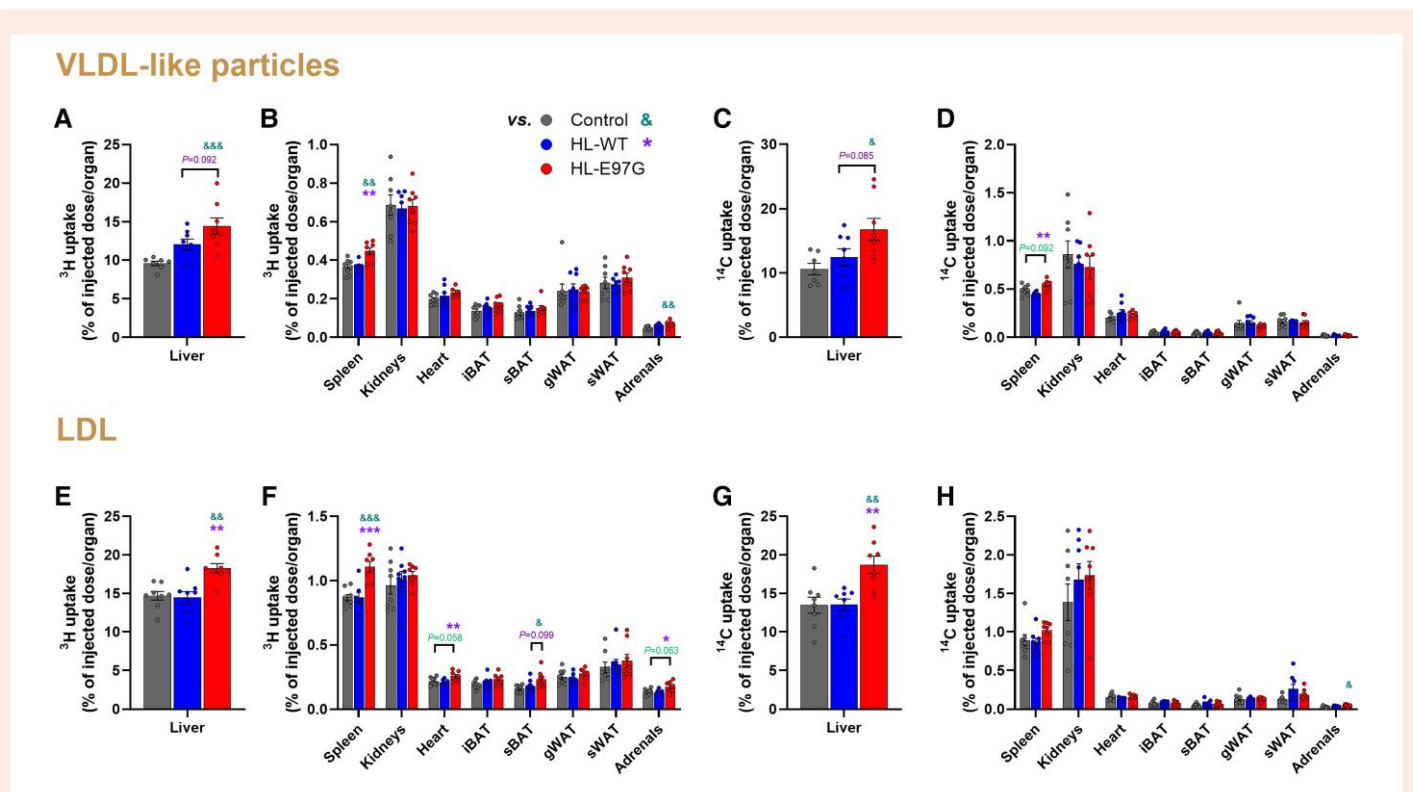


Figure 2 Human HL-E97G expression increases uptake of VLDL uptake by the liver and extrahepatic tissues in *APOE*3-Leiden.CETP* mice. *APOE*3.Leiden.CETP* mice, after 17 weeks of virus injection, were intravenously injected with glycerol tri[^3H]oleate ([^3H]TO) and [^{14}C]cholesteryl oleate ([^{14}C]CO) double-labelled very low density lipoprotein (VLDL)-like particles or LDL. At 15 min after injection of VLDL-like particles, mice were killed and organs/tissues were collected. The activity of ^3H and ^{14}C in the liver (A, C) and other organs/tissues (B, D) were measured. At 30 min after injection of LDL, the activity of ^3H and ^{14}C in the liver (E, G) and other organs/tissues (F, H) were measured. Data are shown as mean \pm S.E.M. ($n = 6\text{--}8/\text{group}$). Differences were assessed using one-way ANOVA with a Tukey correction for multiple comparisons. $\&P < 0.05$, $\&\&P < 0.01$, $\&\&\&P < 0.001$, compared with the HL-WT group. gWAT, gonadal white adipose tissue; iBAT, interscapular brown adipose tissue; sBAT, subscapular brown adipose tissue; sWAT, subcutaneous white adipose tissue.

cholesterol exposure than the HL-E97G variant, and this did not translate into a reduction in atherosclerotic lesions. These data confirm the unique value of the HL-E97G variant for its specific modulation of HL activity.

Regarding the mechanism of action of the HL-E97G variant, we have previously shown that it specifically increases the phospholipase activity of HL, to the detriment of its TG lipase activity, possibly linked to a change in the conformational structure of the lid domain.¹² We observed that HL-E97E lowered HDL-C, without altering its overall composition. Although HDL-C is inversely correlated with ASCVD in humans, Mendelian randomization studies did not provide evidence for a causal role of HDL-C in ASCVD,³⁴ and raising HDL-C by CETP inhibition has been futile with respect to affecting ASCVD outcomes.³⁵ Thus, the reduction of HDL-C by HL-E97G observed in our models is not expected to affect atherosclerosis.

To go further, we performed kinetic experiments using VLDL-like particles and purified human LDL, and we observed that HL-E97G overexpression moderately increases (V)LDL particles hepatic uptake, without substantially affecting peripheral tissue uptake, such as the adipose tissue or the heart. In our previous study, we also performed kinetic experiments on *APOE*3.Leiden.CETP* mice with VLDL-like particles and murine VLDL, and the particles hepatic uptake was not increased in mice overexpressing HL-E97G. Instead, particles uptake was significantly increased in adipose tissue (both white and brown) and oxidative tissues such as the heart or the muscle in the HL-E97G group.¹² On the other hand, this study confirms previous data¹² showing that HL-E97G does not affect either faecal cholesterol or bile acid excretion in *APOE*3.Leiden.CETP*

mice. This apparent discrepancy between our two studies and between the increase in hepatic uptake of (V)LDL and the lack of effect on faecal cholesterol excretion is surprising and still unexplained. Further research is therefore needed to understand in detail the molecular mechanisms underlying the cholesterol-lowering effect of HL-E97G. However, these kinetic experiments in both studies indicate that no significant differences in the tissue clearance profile were observed between the VLDL-like particles (without apoB) and endogenous murine VLDL¹² or human LDL (with apoB) confirming that HL-E97G did not act through an apoB-mediated pathway.

The present results are also encouraging with regard to the positioning of HL-E97G as a new therapeutic target for the management of hypercholesterolaemia. Indeed, it was crucial to verify its effect on the development of atherosclerosis, given that the proband in whom this variant was identified has developed coronary artery disease.¹² It remains unclear however whether such ASCVD was due to altered HL activity or other CV risk factors (the proband had type 2 diabetes and a history of heavy smoking). It is also important to mention that to date, none of the other familial carriers of HL-E97G have reported similar cardiovascular events. The therapeutic benefit of this new cholesterol-lowering mechanism of action mediated by HL-E97G is that it is independent of the action of LDLR, unlike statins or PCSK9 inhibitors. This suggests that it may act synergistically with these classes of LLTs. Above all, it offers future prospects for the therapeutic management of patients with HoFH associated with bi-allelic variants without LDLR activity ('null' alleles). In this group of patients, current therapies are based on LDL-apheresis, evinacumab³⁶ or lomitapide.³⁷ The use of

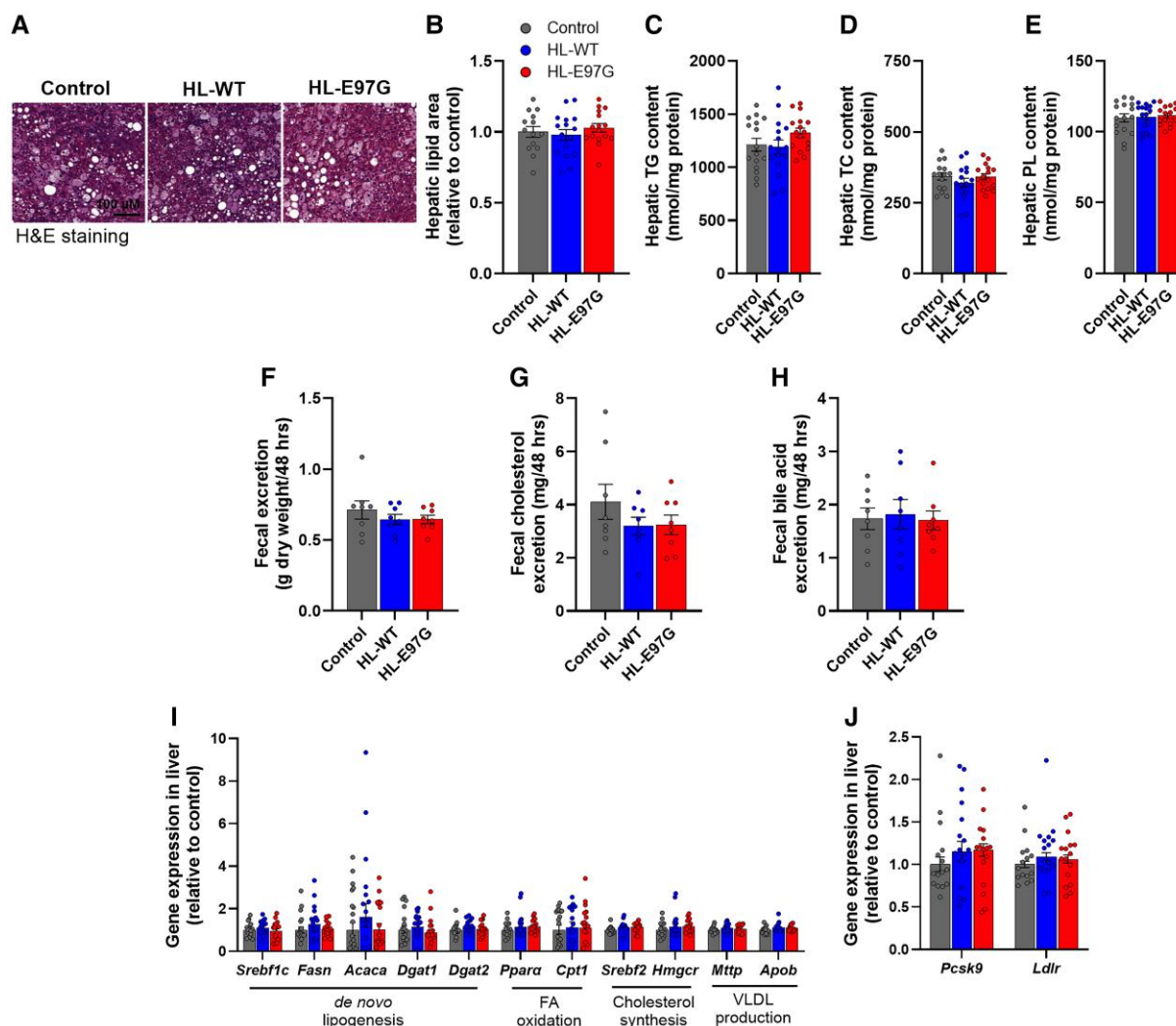


Figure 3 HL-E97G expression does not affect hepatic lipid content and faecal lipid excretion in *APOE*3-Leiden.CETP* mice. At 17 weeks after virus injection into *APOE*3-Leiden.CETP* mice, liver samples were collected and stained with haematoxylin–eosin (H&E; A) and the hepatic lipid area (B) was quantified. Hepatic triglyceride (TG; C), total cholesterol (TC; D), and phospholipid (PL; E) contents were determined. After 10 weeks of virus injection, faeces were collected for 48 h and faecal excretion (F), faecal cholesterol (G), and bile acid (H) excretion were measured. The expression of genes involved in *de novo* lipogenesis synthesis, fatty acid (FA) oxidation, cholesterol synthesis and very low density lipoprotein (VLDL) production (I) and genes involved in lipoprotein uptake (J) was determined in the liver. Data are shown as mean \pm S.E.M. (B–E, I, and J, $n = 14$ –16/group; F–H, $n = 8$ /group). Differences were assessed using one-way ANOVA with a Tukey correction for multiple comparisons. *Acc1*, acetyl coenzyme A carboxylase 1; *Apob*, apolipoprotein B; *Cpt1*, carnitine palmitoyl transferase 1; *Dgat1*, diacylglycerol O-acyltransferase 1; *Dgat2*, diacylglycerol O-acyltransferase 2; *Fasn*, fatty acid synthase; *Hmgcr*, 3-hydroxy-3-methylglutaryl coenzyme A; *Ldlr*, low density lipoprotein receptor; *Mttp*, microsomal triglyceride transfer protein; *Pcsk9*, proprotein convertase subtilisin/kexin type 9; *Ppara*, peroxisome proliferator-activated receptor alpha; *Srebf1c*, sterol regulatory element-binding factor 1c; *Srebf2*, sterol regulatory element-binding factor 2.

lomitapide is limited by the development of liver steatosis, which requires regular liver monitoring, and by significant gastrointestinal disorders, which necessitate the introduction of a long-term low-fat diet.³⁸ Evinacumab, a monoclonal antibody that inhibits the action of ANGPTL3, also acts via an LDLR-independent pathway. In a randomized controlled trial, it has been shown to decrease plasma LDL-C levels of around 50% in HoFH patients, independently of residual LDLR activity.³⁹ Interestingly, recent studies suggested that the LDL-C reduction induced by ANGPTL3 inhibition is associated with an increased EL activity and subsequent accelerated LDL catabolism.^{40,41} Since HL-E97G variant has a lipase activity closer to that of EL, with predominantly phospholipase activity, this underlines the importance of this enzymatic activity in regulating circulating lipoprotein

concentrations. It would therefore be important to determine whether HL-E97G and evinacumab act via common pathways.

In conclusion, this study confirms the potential therapeutic interest of the HL-E97G variant, which is characterized by an increase in HL phospholipase activity, a reduction in circulating lipoproteins without inducing hepatic lipid accumulation and, above all, protection against the development of atherosclerosis in two different mouse models. Its mechanism of action is still under investigation, but implies both a hepatic and extrahepatic pathway, independent of LDLR, to promote lipoprotein catabolism. Together, this study advances our understanding of lipoprotein metabolism and opens up interesting therapeutic perspectives for HoFH patients lacking functional LDLR.

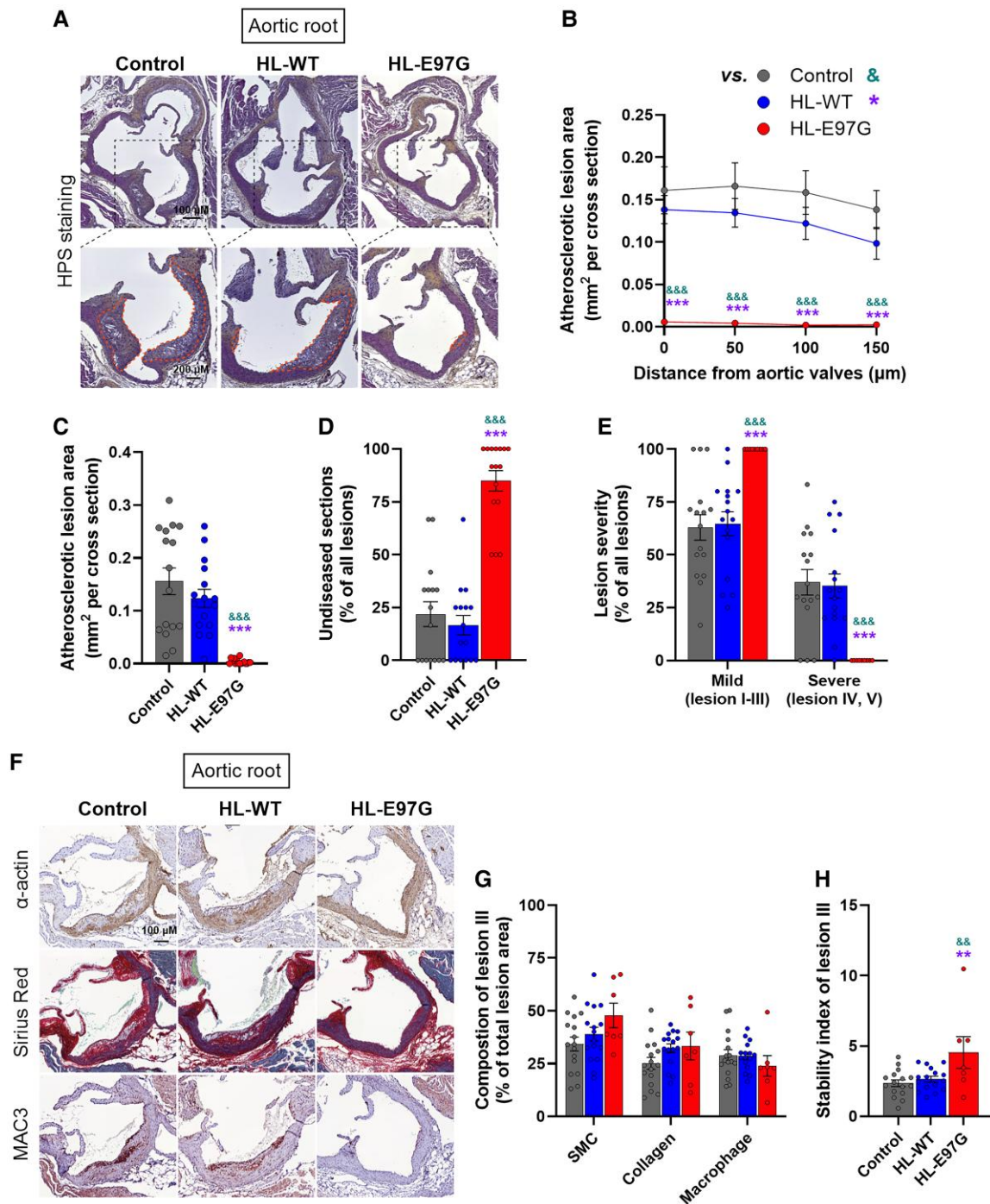


Figure 4 Human HL-E97G expression reduces atherosclerotic area and severity in *APOE*3.Leiden.CETP* mice. At 17 weeks after virus injection into *APOE*3.Leiden.CETP* mice, aortic root samples were collected and stained with haematoxylin phloxine saffron (HPS; A). The atherosclerotic lesion areas of four consecutive sections (with 50 μm intervals) were quantified and plotted as a function of the distance from open aortic valves (B). Average atherosclerotic lesion areas (C) were calculated from B. The undiseased areas were recorded and normalized to total areas (D). Lesions were categorized according to lesion severity, expressed as a percentage of total lesions (E), and shown by lesion severity: mild (types I–III, on the left) and severe (types IV–V, on the right). Representative cross-sections of aortic root labelled with anti-α-smooth muscle cell actin (α-actin), Sirius red and anti-MAC3 antibody (MAC3) were shown (F). The smooth muscle cell, collagen and macrophage areas (G) were quantified in type III lesions and the lesion stability index (i.e. the sum of the smooth muscle cell and collagen area divided by macrophage area) of type III lesions (H) was measured. Data are shown as mean ± S.E.M. (B–D, n = 14–16/group; E, G, and H, n = 16 in control or HL-WT group n = 9 or 7 in HL-E97G group because 7 or 9 mice did not have lesions at all or type III lesions, respectively). Differences were assessed using one-way ANOVA with a Tukey correction for multiple comparisons. &&P < 0.01, &&&P < 0.001, compared with the control group. **P < 0.01, ***P < 0.001, compared with the HL-WT group.

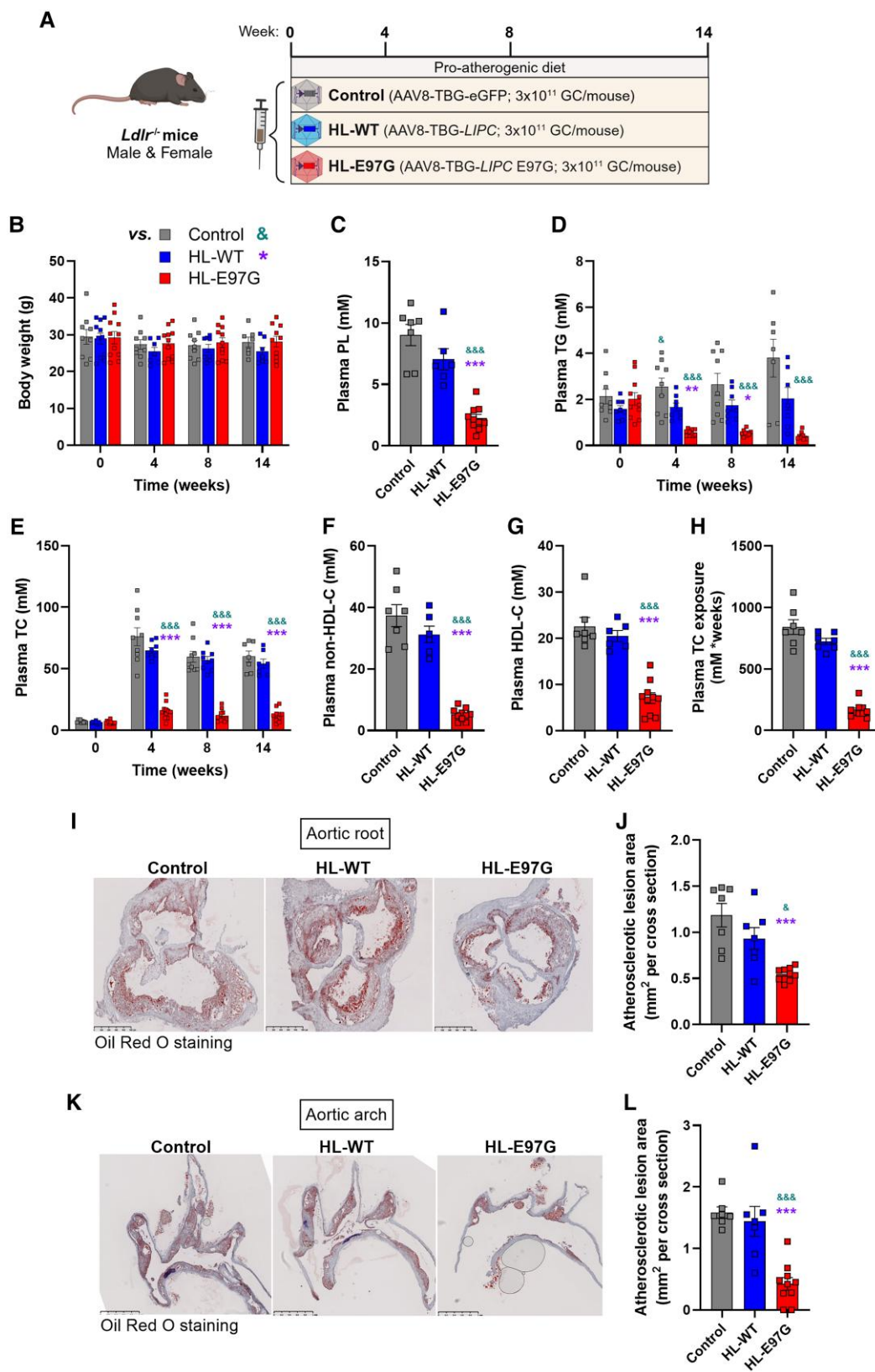


Figure 5 Human HL-E97G expression improves dyslipidaemia and decreases atherosclerotic lesion area in *Ldlr*^{-/-} mice. *Ldlr*^{-/-} mice fed with a pro-atherogenic diet received an intravenous injection with 3 × 10¹¹ genome copies (GC) of adeno-associated viruses (AAV8) expressing either enhanced green fluorescent protein (eGFP; control), the human *LIPC* gene encoding wildtype HL (HL-WT), or the human *LIPC* gene encoding the gain-of-function E97G variant of HL (HL-E97G). Throughout the experimental period, 3 h fasted blood samples were collected to obtain plasma (at Weeks 0, 4, 8, and 14). Mice were killed 14 (continued)

Figure 5 Continued

weeks after virus injection, and the aortic root and arch were collected (A). Body weight (B) was recorded throughout the experimental period. Plasma phospholipid (PL; C) levels were measured at Week 14. Plasma triglyceride (TG; D), and total cholesterol (TC; E) levels throughout the experimental period were determined. Plasma non-high density lipoprotein cholesterol (non-HDL-C; F) and HDL-C (G) levels were measured at Week 14. Plasma TC exposure (H) was calculated from TC levels throughout the experimental period. Representative cross-sections of the aortic root (I) and sagittal section of aortic arch (K) stained with oil red O are shown, and atherosclerotic lesion areas were quantified (J and L). Data are shown as mean \pm S.E.M. ($n = 7$ –10/group). Differences were assessed using one-way ANOVA with a Tukey correction for multiple comparisons. $^{\&}P < 0.05$, $^{\&\&}P < 0.001$, compared with the control group. $^*P < 0.05$, $^{**}P < 0.01$, $^{***}P < 0.001$, compared with the HL-WT group. HL, hepatic lipase.

Translational perspective

Recently, a gain-of-function variant of hepatic lipase (HL-E97G) was identified as a new cause of familial combined hypocholesterolaemia, with reduced plasma LDL-C and HDL-C concentrations. This action is due to a specific increase in the phospholipase activity of HL-E97G. Concordantly, hepatic expression of HL-E97G prevents the development of atherosclerosis in *APOE*3-Leiden.CETP* mice. Importantly, the cholesterol-lowering and anti-atherogenic actions of HL-E97G are independent of the LDL receptor, since they are also exerted in *Ldlr*^{-/-} mice. This opens up promising therapeutic prospects for HL-E97G, particularly in patients with the most severe forms of homozygous familial hypercholesterolaemia with no residual LDLR activity.

Supplementary material

Supplementary material is available at *Cardiovascular Research* online.

Authors' contributions

T.S. and X.G. designed the study, carried out the research, analysed and interpreted the results, and wrote and revised the manuscript. X.G. was responsible for designing, executing, and analysing all experiments with the *APOE*3-Leiden.CETP* mouse model (Figures 1–4; Supplementary material online, Figure S1). M.S., A.T., SF PL, V.L., L.K., A.C.M.P., R.L., T.C.M.S., S.A., W.D., S.S., M.H., N.B., M.G., M.D.F., and P.M. advised the study, carried out the research, analysed, interpreted the results, and reviewed the manuscript. S.K., B.C., P.C.N.R., and C.L.M. designed and advised the study, interpreted the results, edited, reviewed and revised the manuscript, and obtained funding.

Acknowledgements

The authors would like to express their gratitude to Dr Thibaut Quillard, from the Vascular and Pulmonary Diseases team, for his sound and useful advice on the analysis of atherosclerosis in mice. Graphics were created with BioRender.com.

Conflict of interest: none declared.

Funding

This work was supported by the French National Research Agency project CHOPIN (CHolesterol Personalized INnovation) funded by the Agence Nationale de la Recherche (ANR-16-RHUS-0007) and co-ordinated by the CHU of Nantes; the INSTINCTIVE research program funded by the Fondation pour la Recherche Médicale (FRM: EQU201903007846); the HEPALIPA project funded by the Agence Nationale de la Recherche (ANR-R23121NN/RPV23156NNA), the Chinese Scholarship Council (grant 202006850007 to X.G.) and the Netherlands Cardiovascular Research Initiative: an initiative with support of the Dutch Heart Foundation (CVON-GENIUS-2), and the Dutch Heart Foundation (Established Investigator grant 2009T038 to P.C.N.R.).

Data availability

The data underlying this article will be shared on reasonable request to the corresponding authors.

References

- Roth GA, Mensah GA, Johnson CO, Addolorato G, Ammirati E, Baddour LM, Barengo NC, Beaton AZ, Benjamin EJ, Benziger CP, Bonny A, Brauer M, Brodmann M, Cahill TJ, Carapetis J, Catapano AL, Chugh SS, Cooper LT, Coresh J, Criqui M, DeCleene N, Eagle KA, Emmons-Bell S, Feigin VL, Fernández-Solà J, Fowkes G, Gakidou E, Grundy SM, He FJ, Howard G, Hu F, Inker L, Karthikeyan G, Kassebaum N, Koroshetz W, Lavie C, Lloyd-Jones D, Lu HS, Mirijello A, Temesgen AM, Mokdad A, Moran AE, Muntner P, Narula J, Neal B, Ntseke M, Moraes de Oliveira G, Otto C, Owolabi M, Pratt M, Rajagopalan S, Reitsma M, Ribeiro ALP, Rigotti N, Rodgers A, Sable C, Shakil S, Sliwa-Hahnle K, Stark B, Sundström J, Timpel P, Tleyjeh IM, Valgimigli M, Vos T, Whelton PK, Yacoub M, Zuhlke L, Murray C, Fuster V. Global burden of cardiovascular diseases and risk factors, 1990–2019: update from the GBD 2019 study. *J Am Coll Cardiol* 2020;**76**: 2982–3021.
- Vaduganathan M, Mensah GA, Turco JV, Fuster V, Roth GA. The global burden of cardiovascular diseases and risk: a compass for future health. *J Am Coll Cardiol* 2022;**80**:2361–2371.
- Borén J, Chapman MJ, Krauss RM, Packard CJ, Bentzon JF, Binder CJ, Daemen M, Demer LL, Hegele RA, Nicholls SJ, Nordestgaard BG, Watts GF, Bruckert E, Fazio S, Ference BA, Graham I, Horton JD, Landmesser U, Laufs U, Masana L, Pasterkamp G, Raal FJ, Ray KK, Schunkert H, Taskinen MR, van de Sluis B, Wiklund O, Tokgozoglul L, Catapano AL, Ginsberg HN. Low-density lipoproteins cause atherosclerotic cardiovascular disease: pathophysiological, genetic, and therapeutic insights: a consensus statement from the European Atherosclerosis Society Consensus Panel. *Eur Heart J* 2020;**41**:2313–2330.
- Zhang Y, Pletcher MJ, Vittinghoff E, Clemons AM, Jacobs DR Jr, Allen NB, Alonso A, Bellows BK, Oelsner EC, Zeki AI Hazzouri A, Kazi DS, de Ferranti SD, Moran AE. Association between cumulative low-density lipoprotein cholesterol exposure during young adulthood and middle age and risk of cardiovascular events. *JAMA Cardiol* 2021;**6**:1406–1413.
- Mach F, Baigent C, Catapano AL, Koskinas KC, Casula M, Badimon L, Chapman MJ, De Backer GG, Delgado V, Ference BA, Graham IM, Halliday A, Landmesser U, Mihaylova B, Pedersen TR, Riccardi G, Richter DJ, Sabatine MS, Taskinen MR, Tokgozoglul L, Wiklund O. 2019 ESC/EAS Guidelines for the management of dyslipidaemias: lipid modification to reduce cardiovascular risk. *Eur Heart J* 2020;**41**:111–188.
- Ray KK, Molemans B, Schoonen WM, Giovas P, Bray S, Kiru G, Murphy J, Banach M, De Servi S, Gaita D, Gouni-Berthold I, Hovingh GK, Jozwiak JJ, Jukema JW, Kiss RG, Kownator S, Iversen HK, Maher V, Masana L, Parkhomenko A, Peeters A, Clifford P, Raslova K, Siostrzonek P, Romeo S, Tousoulis D, Vlachopoulos C, Vrablik M, Catapano AL, Poulter NR. EU-wide cross-sectional observational study of lipid-modifying therapy use in secondary and primary care: the DA VINCI study. *Eur J Prev Cardiol* 2021;**28**:1279–1289.
- Ray KK, Haq I, Bilitou A, Manu MC, Burden A, Aguiar C, Arca M, Connolly DL, Eriksson M, Ferrières J, Laufs U, Mostaza JM, Nanchen D, Rietzschel E, Strandberg T, Toplak H, Visseren FLJ, Catapano AL. Treatment gaps in the implementation of LDL cholesterol control among high- and very high-risk patients in Europe between 2020 and 2021: the multinational observational SANTORINI study. *Lancet Reg Health Eur* 2023;**29**:100624.

8. Tromp TR, Hartgers ML, Hovingh GK, Vallejo-Vaz AJ, Ray KK, Soran H, Freiburger T, Bertolini S, Harada-Shiba M, Blom DJ, Raal FJ, Cuchel M. Worldwide experience of homozygous familial hypercholesterolaemia: retrospective cohort study. *Lancet* 2022;**399**: 719–728.
9. Raal FJ, Hegele RA, Ruzza A, López JAG, Bhatia AK, Wu J, Wang H, Gaudet D, Wiegman A, Wang J, Santos RD. Evolocumab treatment in pediatric patients with homozygous familial hypercholesterolemia: pooled data from three open-label studies. *Arterioscler Thromb Vasc Biol* 2024;**44**:1156–1164.
10. Gu J, Gupta RN, Cheng HK, Xu Y, Raal FJ. Current treatments for the management of homozygous familial hypercholesterolaemia: a systematic review and commentary. *Eur J Prev Cardiol* 2024;**31**:1833–1849.
11. Raal FJ, Rosenson RS, Reeskamp LF, Hovingh GK, Kastelein JJP, Rubba P, Ali S, Banerjee P, Chan KC, Gipe DA, Khilli N, Pordy R, Weinreich DM, Yancopoulos GD, Zhang Y, Gaudet D. Evinacumab for homozygous familial hypercholesterolemia. *N Engl J Med* 2020;**383**:711–720.
12. Dijk W, Di Filippo M, Kooijman S, van Eenige R, Rimbert A, Caillaud A, Thedrez A, Arnaud L, Pronk A, Garçon D, Sotin T, Lindenbaum P, Ozcariz Garcia E, Pais de Barros JP, Duvallard L, Si-Tayeb K, Amigo N, Le Questel JY, Rensen PCN, Le May C, Moulin P, Cariou B. Identification of a gain-of-function LIPC variant as a novel cause of familial combined hypocholesterolemia. *Circulation* 2022;**146**:724–739.
13. Santamarina-Fojo S, González-Navarro H, Freeman L, Wagner E, Nong Z. Hepatic lipase, lipoprotein metabolism, and atherogenesis. *Arterioscler Thromb Vasc Biol* 2004;**24**: 1750–1754.
14. van Vlijmen BJ, van 't Hof HB, Mol MJ, van der Boom H, van der Zee A, Frants RR, Hofker MH, Havekes LM. Modulation of very low density lipoprotein production and clearance contributes to age- and gender- dependent hyperlipoproteinemia in apolipoprotein E3-Leiden transgenic mice. *J Clin Invest* 1996;**97**:1184–1192.
15. van Eenige R, Verhave PS, Koemans PJ, Tiebosch I, Rensen PCN, Kooijman S. RandoMice, a novel, user-friendly randomization tool in animal research. *PLoS One* 2020;**15**:e0237096.
16. In Het Panhuis W, Kooijman S, Brouwers B, Verhoeven A, Pronk ACM, Streefland TCM, Giera M, Schrauwen P, Rensen PCN, Schönke M. Mild exercise does not prevent atherosclerosis in APOE*3-Leiden.CETP mice or improve lipoprotein profile of men with obesity. *Obesity (Silver Spring)* 2020;**28**:S93–s103.
17. van Eenige R, Ying Z, Tambyrajah L, Pronk ACM, Blomberg N, Giera M, Wang Y, Coskun T, van der Stelt M, Rensen PCN, Kooijman S. Cannabinoid type 1 receptor inverse agonism attenuates dyslipidemia and atherosclerosis in APOE*3-Leiden.CETP mice. *J Lipid Res* 2021;**62**:100070.
18. Bligh EG, Dyer WJ. A rapid method of total lipid extraction and purification. *Can J Biochem Physiol* 1959;**37**:911–917.
19. Wong MC, van Diepen JA, Hu L, Guigas B, de Boer HC, van Puijvelde GH, Kuiper J, van Zonneveld AJ, Shoelson SE, Voshol PJ, Romijn JA, Havekes LM, Tamsma JT, Rensen PC, Hiemstra PS, Berbee JF. Hepatocyte-specific IKK β expression aggravates atherosclerosis development in APOE*3-Leiden mice. *Atherosclerosis* 2012;**220**:362–368.
20. van der Vaart JI, van Eenige R, Rensen PCN, Kooijman S. Atherosclerosis: an overview of mouse models and a detailed methodology to quantify lesions in the aortic root. *Vasc Biol* 2024;**6**:e230017.
21. Bessueille L, Kawthary L, Quillard T, Goetsch C, Briolay A, Taraconat N, Balayssac S, Gilard V, Mebarek S, Peyruchaud O, Duboeuf F, Bouillot C, Pinkerton A, Mechtouf L, Buchet R, Hamade E, Zibara K, Fonta C, Canet-Soulas E, Millan JL, Magne D. Inhibition of alkaline phosphatase impairs dyslipidemia and protects mice from atherosclerosis. *Transl Res* 2023;**251**:2–13.
22. Mehlem A, Hagberg CE, Muhl L, Eriksson U, Falkevall A. Imaging of neutral lipids by oil red O for analyzing the metabolic status in health and disease. *Nat Protoc* 2013;**8**:1149–1154.
23. Jansen H, Verhoeven AJ, Sijbrands EJ. Hepatic lipase: a pro- or anti-atherogenic protein? *J Lipid Res* 2002;**43**:1352–1362.
24. Zambon A, Deeb SS, Hokanson JE, Brown BG, Brunzell JD. Common variants in the promoter of the hepatic lipase gene are associated with lower levels of hepatic lipase activity, buoyant LDL, and higher HDL2 cholesterol. *Arterioscler Thromb Vasc Biol* 1998;**18**: 1723–1729.
25. Connelly PW, Hegele RA. Hepatic lipase deficiency. *Crit Rev Clin Lab Sci* 1998;**35**:547–572.
26. Dichek HL, Brecht W, Fan J, Ji ZS, McCormick SP, Akeefe H, Conzo L, Sanan DA, Weisgraber KH, Young SG, Taylor JM, Mahley RW. Overexpression of hepatic lipase in transgenic mice decreases apolipoprotein B-containing and high density lipoproteins. Evidence that hepatic lipase acts as a ligand for lipoprotein uptake. *J Biol Chem* 1998;**273**: 1896–1903.
27. Dichek HL, Johnson SM, Akeefe H, Lo GT, Sage E, Yap CE, Mahley RW. Hepatic lipase overexpression lowers remnant and LDL levels by a noncatalytic mechanism in LDL receptor-deficient mice. *J Lipid Res* 2001;**42**:201–210.
28. Freeman L, Amar MJ, Shamburek R, Paigen B, Brewer HB Jr, Santamarina-Fojo S, González-Navarro H. Lipolytic and ligand-binding functions of hepatic lipase protect against atherosclerosis in LDL receptor-deficient mice. *J Lipid Res* 2007;**48**:104–113.
29. Knudsen P, Antikainen M, Uusi-Oukari M, Ehnholm S, Lahdenperä S, Bensaadoun A, Funke H, Wiebusch H, Assmann G, Taskinen MR, Ehnholm C. Heterozygous hepatic lipase deficiency, due to two missense mutations R186H and L334F, in the HL gene. *Atherosclerosis* 1997;**128**: 165–174.
30. Dugi KA, Brandauer K, Schmidt N, Nau B, Schneider JG, Mentz S, Keiper T, Schaefer JR, Meissner C, Kather H, Bahner ML, Fiehn W, Kreuzer J. Low hepatic lipase activity is a novel risk factor for coronary artery disease. *Circulation* 2001;**104**:3057–3062.
31. Silbernagel G, Scharnagl H, Kleber ME, Delgado G, Stojakovic T, Laaksonen R, Erdmann J, Rankinen T, Bouchard C, Landmesser U, Schunkert H, März W, Grammer TB. LDL triglycerides, hepatic lipase activity, and coronary artery disease: an epidemiologic and Mendelian randomization study. *Atherosclerosis* 2019;**282**:37–44.
32. Johannsen TH, Kamstrup PR, Andersen RV, Jensen GB, Sillesen H, Tybjaerg-Hansen A, Nordestgaard BG. Hepatic lipase, genetically elevated high-density lipoprotein, and risk of ischemic cardiovascular disease. *J Clin Endocrinol Metab* 2009;**94**:1264–1273.
33. Fan YM, Raitakari OT, Kähönen M, Hutri-Kähönen N, Juonala M, Marniemi J, Viikari J, Lehtimäki T. Hepatic lipase promoter C-480T polymorphism is associated with serum lipids levels, but not subclinical atherosclerosis: the Cardiovascular Risk in Young Finns Study. *Clin Genet* 2009;**76**:46–53.
34. Voight BF, Peloso GM, Orho-Melander M, Frikke-Schmidt R, Barbalic M, Jensen MK, Hindy G, Hólm H, Ding EL, Johnson T, Schunkert H, Samani NJ, Clarke R, Hopewell JC, Thompson JF, Li M, Thorleifsson G, Newton-Cheh C, Musunuru K, Pirruccello JP, Saleheen D, Chen L, Stewart A, Schillert A, Thorsteinsdottir U, Thorgeirsson G, Anand S, Engert JC, Morgan T, Spertus J, Stoll M, Berger K, Martinelli N, Girelli D, McKeown PP, Patterson CC, Epstein SE, Devaney J, Burnett MS, Mooser V, Ripatti S, Surakka I, Nieminen MS, Sinisalo J, Lokki ML, Perola M, Havulinna A, de Faire U, Gigante B, Ingelsson E, Zeller T, Wild P, de Bakker PI, Klungel OH, Maitland-van der Zee AH, Peters BJ, de Boer A, Grobbee DE, Kamphuisen PW, Deneer VH, Elbers CC, Onland-Moret NC, Hofker MH, Wijmenga C, Verschuren WM, Boer JM, van der Schouw YT, Rasheed A, Frossard P, Demissie S, Willer C, Do R, Ordovas JM, Abecasis GR, Boehnke M, Mohlke KL, Daly MJ, Guiducci C, Burtt NP, Surti A, Gonzalez E, Purcell S, Gabriel S, Marrugat J, Peden J, Erdmann J, Diemert P, Willenborg C, König IR, Fischer M, Hengstenberg C, Ziegler A, Buyschaert I, Lambrechts D, Van de Werf F, Fox KA, El Mokhtari NE, Rubin D, Schrezenmeir J, Schreiber S, Schäfer A, Danesh J, Blankenberg S, Roberts R, McPherson R, Watkins H, Hall AS, Overvad K, Rimm E, Boerwinkle E, Tybjaerg-Hansen A, Cupples LA, Reilly MP, Melander O, Mannucci PM, Ardissino D, Siscovick D, Elosua R, Stefansson K, O'Donnell CJ, Salomaa V, Rader DJ, Peltonen L, Schwartz SM, Altschuler D, Kathiresan S. Plasma HDL cholesterol and risk of myocardial infarction: a Mendelian randomisation study. *Lancet* 2012;**380**:572–580.
35. Lincoff AM, Nicholls SJ, Riesmeyer JS, Barter PJ, Brewer HB, Fox KAA, Gibson CM, Granger C, Menon V, Montalescot G, Rader D, Tall AR, McRlean E, Wolski K, Ruotolo G, Vangerow B, Weerakkody G, Goodman SG, Conde D, McGuire DK, Nicolau JC, Leiva-Pons JL, Pesant Y, Li W, Kandath D, Kouz S, Tahirkheli N, Mason D, Nissen SE. Evacetrapib and cardiovascular outcomes in high-risk vascular disease. *N Engl J Med* 2017;**376**:1933–1942.
36. Béliard S, Saheb S, Litzler-Renault S, Vimont A, Valero R, Bruckert É, Farnier M, Gallo A. Evinacumab and cardiovascular outcome in patients with homozygous familial hypercholesterolemia. *Arterioscler Thromb Vasc Biol* 2024;**44**:1447–1454.
37. Cuchel M, Raal FJ, Hegele RA, Al-Rasadi K, Arca M, Averna M, Bruckert E, Freiburger T, Gaudet D, Harada-Shiba M, Hudgins LC, Kayikcioglu M, Masana L, Parhofer KG, Roeters van Lennepe JE, Santos RD, Stroes ESG, Watts GF, Wiegman A, Stock JK, Tokgözoğlu LS, Catapano AL, Ray KK. 2023 update on European Atherosclerosis Society consensus statement on homozygous familial hypercholesterolaemia: new treatments and clinical guidance. *Eur Heart J* 2023;**44**:2277–2291.
38. Ben-Omran T, Masana L, Kolovou G, Ariceta G, Nóvoa FJ, Lund AM, Bogsrud MP, Araujo M, Hussein O, Ibarretxe D, Sanchez-Hernández RM, Santos RD. Real-world outcomes with lomitapide use in paediatric patients with homozygous familial hypercholesterolaemia. *Adv Ther* 2019;**36**:1786–1811.
39. Raal FJ, Rosenson RS, Reeskamp LF, Kastelein JJP, Rubba P, Duell PB, Koseki M, Stroes E, Ali S, Banerjee P, Chan KC, Khilli N, McGinniss J, Pordy R, Zhang Y, Gaudet D. The long-term efficacy and safety of evinacumab in patients with homozygous familial hypercholesterolemia. *JACC Adv* 2023;**2**:100648.
40. Adam RC, Mintah IJ, Alexa-Braun CA, Shihanian LM, Lee JS, Banerjee P, Hamon SC, Kim HI, Cohen JC, Hobbs HH, Van Hout C, Gromada J, Murphy AJ, Yancopoulos GD, Sleeman MW, Gusarova V. Angiotensin-like protein 3 governs LDL-cholesterol levels through endothelial lipase-dependent VLDL clearance. *J Lipid Res* 2020;**61**:1271–1286.
41. Wu L, Soundarapandian MM, Castoreno AB, Millar JS, Rader DJ. LDL-cholesterol reduction by ANGPTL3 inhibition in mice is dependent on endothelial lipase. *Circ Res* 2020;**127**: 1112–1114.